doi.org/10.26434/chemrxiv.14152316.v1

Development of an Amino Sugar-Based Supramolecular Hydrogelator with Reduction Responsiveness

Sayuri L. Higashi, Masato Ikeda

Submitted date: 03/03/2021 • Posted date: 04/03/2021

Citation information: Higashi, Sayuri L.; Ikeda, Masato (2021): Development of an Amino Sugar-Based Supramolecular Hydrogelator with Reduction Responsiveness. ChemRxiv. Preprint. https://doi.org/10.26434/chemrxiv.14152316.v1

Stimuli-responsive supramolecular hydrogels are a newly emerging class of aqueous soft materials with a wide variety of bioapplications. Here we report a reduction-responsive supramolecular hydrogel constructed from a markedly simple low-molecular-weight hydrogelator, which is developed on the basis of modular molecular design containing a hydrophilic amino sugar and a reduction-responsive nitrophenyl group. The hydrogel formation ability differs significantly between glucosamine- and galactosamine-based self-assembling molecules, which are epimers at the C4 position, and only the glucosamine-based derivative can act as a hydrogelator.

Development of an amino sugar-based supramolecular hydrogelator with reduction responsiveness

Sayuri L. Higashi[1] and Masato Ikeda[1,2,3,4,5]*

[1] *United Graduate School of Drug Discovery and Medical Information Sciences, Gifu University, 1-1 Yanagido, Gifu 501-1193, Japan*

[2] *Department of Chemistry and Biomolecular Science, Faculty of Engineering, Gifu University, 1-1 Yanagido, Gifu 501-1193, Japan*

[3] *Center for Highly Advanced Integration of Nano and Life Sciences, Gifu University (G-CHAIN), 1-1 Yanagido, Gifu 501-1193, Japan*

[4] *Institute of Nano-Life-Systems, Institutes of Innovation for Future Society, Nagoya University, Furo-cho, Chikusa-ku, Nagoya, 464-8603, Japan*

[5] *Institute for Glyco-core Research (iGCORE), Gifu University, Furo-cho, Chikusa-ku, Nagoya, 464-8603, Japan*

*Correspondence: m_ikeda@gifu-u.ac.jp, orcid.org/0000-0003-4097-829

Table of Contents

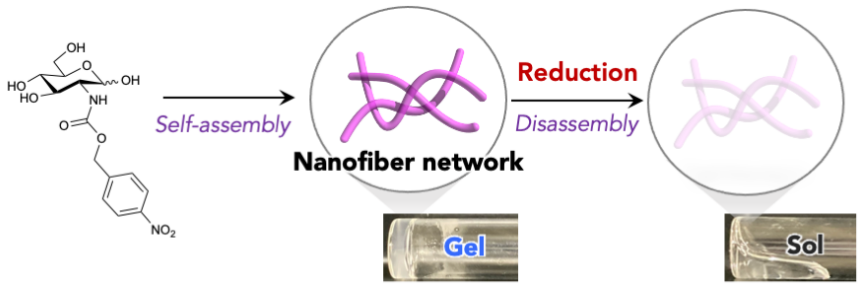

ABSTRACT: Stimuli-responsive supramolecular hydrogels are a newly emerging class of aqueous soft materials with a wide variety of bioapplications. Here we report a reduction-responsive supramolecular hydrogel constructed from a markedly simple low-molecular-weight hydrogelator, which is developed on the basis of modular molecular design containing a hydrophilic amino sugar and a reduction-responsive nitrophenyl group. The hydrogel formation ability differs significantly between glucosamine- and galactosamine-based self-assembling molecules, which are epimers at the C4 position, and only the glucosamine-based derivative can act as a hydrogelator.

KEYWORDS: supramolecular hydrogel, low-molecular-weight hydrogelator, reduction responsiveness, amino sugar, nitrophenyl group

INTRODUCTION

Supramolecular hydrogels,[1] which consist of a network of supramolecular nanoarchitectures built from supramolecular hydrogelators (or low-molecular-weight hydrogelators), can be used in a variety of bioapplications, such as drug releasing matrices,[2] sensing materials,[3] and cell-culturing or cell-killing materials.[4] Because supramolecular hydrogels are readily constructed from chemically well-defined supramolecular hydrogelators, various functions can be installed into them, including responsiveness toward specific stimuli, such as pH,[5] light,[6] and redox,[7] via a semirational, albeit not always predictable, molecular design of the supramolecular hydrogelators.

In this context, the development of reduction-responsive supramolecular hydrogels through semirational molecular design has recently attracted attention[7] because the reduction stimuli can be biocompatible and the dysregulation of reductive conditions in living organisms is known to be associated with certain diseases such as cancer.[8] Specifically, the introduction of a disulfide linkage is considered the most reliable molecular design[7a-c] because this linkage can be readily cleaved under reductive conditions generated upon the addition of reducing agents, such as phosphine derivatives, or in the presence of biorelevant and biocompatible thiols, such as reduced glutathione. In fact, dibenzoyl cysteine, a long-known supramolecular hydrogelator containing a disulfide linkage,[7a] exhibits reduction-responsive gel-to-sol transition.[7c] Other reduction-sensitive chemical groups, such as azo,[7d] ferrocenoyl,[7e] phenylselenyl,[7f] and nitro groups,[7g] have also been effectively utilized to develop reduction-responsive supramolecular hydrogels.

For the design of self-assembling molecules including supramolecular hydrogelators, carbohydrates are attractive owing to not only the presence of multiple hydrophilic hydroxyl groups to modulate the amphiphilic tendency but also their inherent chirality, which facilitates the asymmetric arrangement of the self-assembling molecules to form fibrous supramolecular nanoarchitectures suitable for hydrogel formation.[9,10] In particular, amino sugars including galactosamine ($GalNH_2$: 2-amino-2-deoxy-D-galactose) and glucosamine ($GlcNH_2$:

2-amino-2-deoxy-D-glucose), which are major components of structural polysaccharides present on the surface of mammalian cells,[11] are useful because they possess a single amino group at the C2 position that serves as an anchor site for the simple and selective conjugation with a variety of functionalities conducive to the self-assembly behavior, including aromatic amino acids and alkyl chains.[12] For instance, Birchall *et al*. recently reported simple supramolecular hydrogelators derived from amino sugars bearing the fluorenyl-9-methoxycarbonyl (Fmoc) group as a powerful self-assembly facilitating group (referred to as **GalN-** and **GlcN-Fmoc** in **Figure 1**).[13] Following this line, we herein report that the introduction of a 4-nitrophenylmethoxycarbonyl (NPmoc) group, instead of Fmoc, into one of such amino sugars gives rise to a supramolecular hydrogelator (**GlcN-NPmoc**, **Figure 1**), which is more compact than its Fmoc counterpart (M_w = 358.30 g/mol for **GlcN-NPmoc** vs. M_w = 401.42 g/mol for **GlcN-Fmoc**) and, unlike the latter, exhibits the desired reduction-responsive function. The newly developed **GlcN-NPmoc**, which is a purely organic compound without any transition metal, is one of the simplest low-molecular-weight supramolecular hydrogelators capable of producing reduction-responsive functional supramolecular hydrogels reported to date (**Figure S1**).[14]

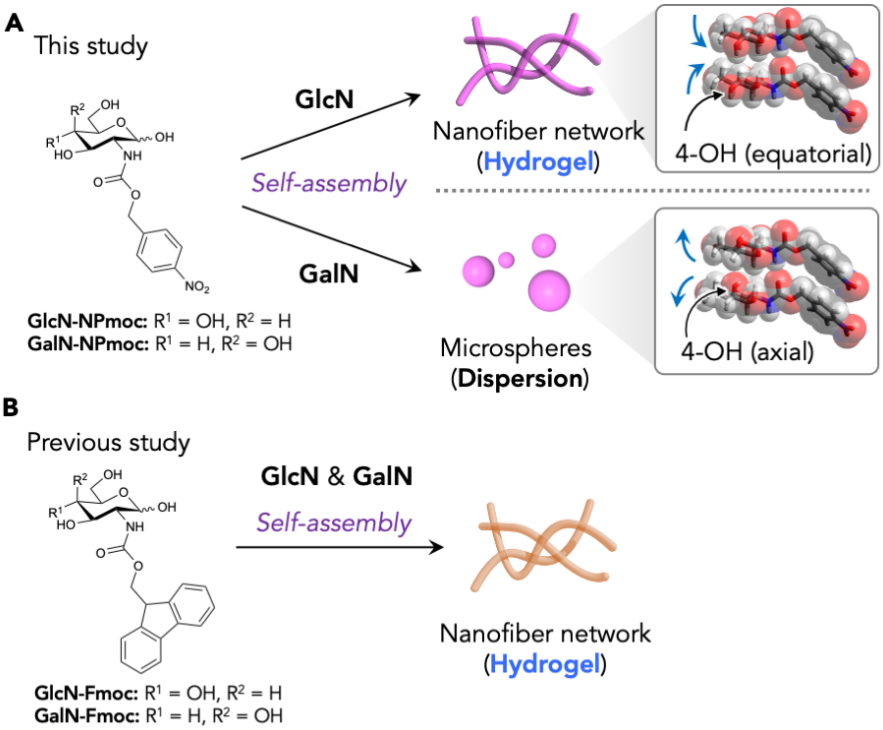

Figure 1. (**A**) Chemical structures and schematic representation of the self-assembly of **GlcN-** and **GalN-NPmoc** into a nanofiber network and microspheres, respectively, investigated in this study. The insets on the right-hand side represent possible molecular models for the self-assembled structures. Possibility of anti-parallel and interdigitated self-assembled structures (not presented) should not be excluded.[13a] (**B**) Chemical structures of **GlcN-** and **GalN-Fmoc** reported previously by Birchall *et al*.[13a]

RESULTS AND DISCUSSION

A straightforward synthesis of NPmoc-carbohydrates, **GlcN-** and **GalN-NPmoc**, was carried out according to a previously reported method (**Scheme S1**).[13a,15] To evaluate the aqueous self-assembling ability of **GlcN-** and **GalN-NPmoc**, their stock solutions in dimethyl sulfoxide (DMSO), a water-miscible organic solvent, were mixed with an aqueous buffer, i.e., 100 mM 4-(2-hydroxyethyl)-1-piperazineethanesulfonic acid (HEPES)–NaOH (pH 7.4). The resultant suspensions were heated to obtain clear solutions and then cooled to room temperature to induce the self-assembly. We found that **GlcN-NPmoc** formed a stable hydrogel above a concentration of approximately 0.75 wt% (21 mM), whereas **GalN-NPmoc** only produced suspensions (no gel formation was observed even at higher concentrations, e.g., 1.0 wt%), as shown in **Figure 2A**. Also, the powders of **GlcN-NPmoc** were directly mixed with aqueous media [e.g., HEPES–NaOH (pH 7.4) or MES-NaOH (pH 5.5)], phosphate buffered saline, milli-Q water, or deuterium oxide (D_2O). Similar heating/cooling treatment of the suspensions gave stable hydrogels and the hydrogel prepared with D_2O was used for Fourier transform infrared (FTIR) and nuclear magnetic resonance (NMR) spectroscopy study (*vide infra*). The viscoelastic property of the representative **GlcN-NPmoc** hydrogels was evaluated through conventional oscillatory rheology experiments (**Figure 2B**), which indicated the formation of physical hydrogels.[16] The **GlcN-NPmoc** hydrogels were stable for several weeks whereas showed no thixotropy, i.e., no recovery of the original gel state after mechanical breakdown. Nonetheless, the formation of the **GlcN-NPmoc** hydrogels was thermally reversible and the gel-to-sol transition temperature (T_{gel}) was determined to be 51 °C for a hydrogel concentration of 1.0 wt% in 100 mM HEPES–NaOH (pH 7.4) with DMSO (5.0 vol%). Note that the difference in the hydrogel formation ability between glucosamine-based **GlcN-NPmoc** and galactosamine-based **GalN-NPmoc**, which are epimers at the C4 position of the amino sugar, contrasts with the previous report on Fmoc hydrogels, in which both derivatives (**GlcN-** and **GalN-Fmoc**) demonstrated hydrogel formation ability.[13a] We presume that the axial OH group at the C4 position in the GalN group of **GalN-NPmoc** may hinder the formation of self-assembled network structures (nanofiber network, *vide infra*), which is required for hydrogel formation. **Figure 1A** depicts a plausible model for the self-assembled structures. We speculate that the strong tendency of the Fmoc group in **GalN-Fmoc** to induce the one-dimensional self-assembly[17] compared with the less hydrophobic and smaller aromatic NPmoc group may overcome the hampering effect of the axial OH group in the pyranose ring.

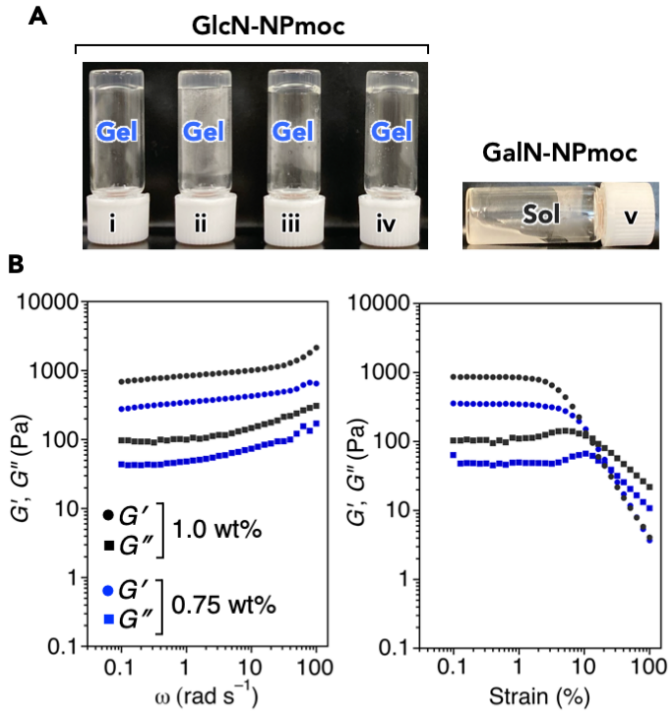

Figure 2. (**A**) Photographs of **GlcN-NPmoc** hydrogels prepared using 100 mM HEPES–NaOH (pH 7.4) (**i**) with or (**ii**) without DMSO (5.0 vol%), (**iii**) milli-Q water, (**iv**) phosphate buffered saline, and (**v**) a **GalN-NPmoc** dispersion (sol) prepared using 100 mM HEPES–NaOH (pH 7.4) containing DMSO (5.0 vol%). [**GlcN-** or **GalN-NPmoc**] = 0.75 wt%. Please see **Figure S6** for more details. (**B**) Frequency and strain sweep (0.20% stain for frequency sweep and 1.0 rad s^{-1} for strain sweep) rheological properties of **GlcN-NPmoc** hydrogels {[**GlcN-NPmoc**] = 0.75 and 1.0 wt%, 100 mM HEPES–NaOH (pH 7.4) containing DMSO (5.0 vol%): *G′*, storage modulus; *G″*, loss modulus} at 25 °C.

To investigate the morphology of the self-assembled structures, transmission electron microscopy (TEM) observations were performed. As shown in **Figure 3A_i**, **GlcN-NPmoc** produced nanofiber networks, which is characteristic of supramolecular hydrogels.[1,7,10] Meanwhile, **GalN-NPmoc** formed nonnetworked spherical structures, as seen in **Figure 3A_ii**. This obvious morphological difference is consistent with their distinct hydrogel formation ability. To probe the morphology without drying the samples, the **GlcN-NPmoc** hydrogel and **GalN-NPmoc** sol were subjected to in situ confocal laser scanning microscopy (CLSM) observation. Upon the addition of Nile Red as a typical hydrophobic fluorescent probe,[10k] an aggregated fibrous network and spherical structures were visualized for **GlcN-** and **GalN-NPmoc**, respectively, as shown in **Figure 3B**. The smaller average size of the spherical structures of **GalN-NPmoc** (1.8 ± 0.8 μm) in the TEM images compared with that in the CLSM images (2.5 ± 1.4 μm) could be ascribed to the influence of drying the sample for the TEM observations. Interestingly, we found that similar structures were observed with CLSM when using a fluorescent

probe bearing a hydrazide group (4-hydrazino-7-nitro-2,1,3-benzoxadiazole, NBD-H), as presented in **Figure S7**, which can be attributed to the formation of a hydrazone bond between NBD-H and the nonreducing end of the sugar moiety in **GlcN-** and **GalN-NPmoc**.[18] This reactivity has been scarcely explored for this class of sugar-based self-assembling molecules because most of them lack a nonreducing end in the sugar moiety, which enabled post-self-assembly functionalization of the present supramolecular architecture via dynamic covalent chemistry.[19]

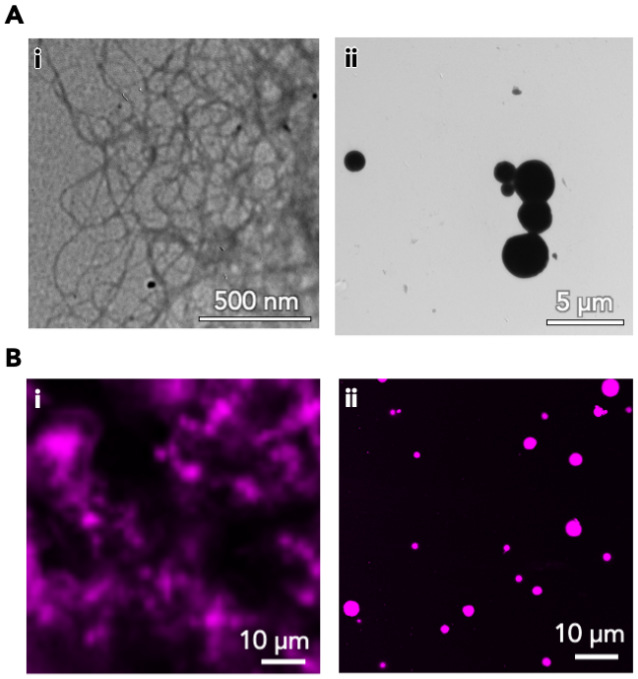

Figure 3. Representative (**A**) TEM and (**B**) CLSM images of (**i**) the **GlcN-NPmoc** hydrogel and (**ii**) the **GalN-NPmoc** dispersion (sol). Details on the CLSM observation protocols are described in supporting information.

To gain further insight into the present system and elucidate the self-assembly mode of **GlcN-NPmoc** in the hydrogel state, spectroscopic studies were conducted. As shown in **Figures 4** and **S8**, the circular dichroism (CD) spectrum of the **GlcN-NPmoc** hydrogel displayed a bisignate CD signal with a negative peak at 286 nm and a positive peak at 258 nm, which is assignable to an exciton coupling between individual π–π* transitions of the nitrophenyl group centered at 276 nm (λ_{max}). This putatively assigned negative exciton CD couplet suggests negative chirality for the asymmetric arrangement (preferably left-handed) of the nitrophenyl moiety in the self-assembled state. In addition, the FTIR spectrum of the **GlcN-NPmoc** hydrogel (prepared with D_2O at 3.0 wt% concentration) showed a distinct peak assignable to carbonyl stretching of the carbamate bond of the NPmoc group at 1664 cm^{-1} (**Figure S9**), which is shifted to a slightly lower energy compared with that of an

NPmoc-containing water-soluble compound (see supporting information for details) appearing at 1685 cm^{-1}. This suggests the importance of hydrogen bonding interactions in the self-assembled structures of **GlcN-NPmoc**. Collectively, these results are consistent with the plausible model of self-assembled **GlcN-NPmoc** as fibrous nanostructures in the hydrogel state proposed above (**Figure 1A**).

With this new nitro group-containing supramolecular hydrogelator based on an amino sugar (**GlcN-NPmoc** hydrogel) in hand, we next investigated its reduction-responsive property. By carefully adding an aqueous solution (100 μL) containing $Na_2S_2O_4$ as a chemical reductant (20 eq. against **GlcN-NPmoc**) onto the **GlcN-NPmoc** hydrogel (1.0 wt%, 28 mM, 100 μL), macroscopic gel-to-sol transition (gel degradation) was observed within 30 min at room temperature, as shown in **Figure 4A**. In contrast, upon the addition of the same amount of nonreductant Na_2SO_4, no gel degradation was observed, suggesting that the influence of increased salt concentration on the $Na_2S_2O_4$-induced gel degradation was not significant. Moreover, the addition of tris(2-carboxyethyl)phosphine hydrochloride (TCEP, 1.0 eq. against **GlcN-NPmoc**) in an amount that would be sufficient to induce the cleavage of disulfide bonds according to a recent report[7c] did not induce gel degradation. Collectively, these results indicate that the $Na_2S_2O_4$-induced gel degradation correlates with the chemical reduction of the nitro group, whose selectivity is consistent with previous reports.[7g] The CD spectrum recorded 30 min after the addition of $Na_2S_2O_4$ showed that the original bisignate CD signal (**Figure 4B**) virtually disappeared, which was associated with the disappearance of the absorption peak at ~276 nm assignable to the nitrophenyl group (**Figure S8**). In addition, CLSM observations revealed the evanescence of the aggregated fibrous network within 30 min after the addition of $Na_2S_2O_4$ (**Figure 4C**). The reduction response, i.e., the reduction of the nitro group, of **GlcN-NPmoc** induced by $Na_2S_2O_4$ was further investigated by ^{1}H NMR spectroscopy (**Figure S10**), which was conducted after dissolution of the samples in DMSO-d_6 (for a gel prepared with D_2O and sol after $Na_2S_2O_4$-induced gel degradation, a similar responsiveness was validated). We found that the signals attributable to the NPmoc group (nitrophenyl and benzyl protons) almost completely disappeared after the $Na_2S_2O_4$-induced gel degradation, whereas new multiple peaks assignable to (hydroxyl)aminophenyl groups (~6.5–7.3 ppm) appeared. The presence of other new multiple peaks in the region ~4.7–4.9 ppm, which could be assigned to benzylic protons, suggests that several compounds were generated most probably through the reaction between quinoneimine methide (released from **GlcN-NPmoc** via reduction-triggered 1,6-elimination) and nucleophiles including water molecule and the amino group of the generated glucosamine. Furthermore, the appearance of other peaks at 9.96 and 8.32 ppm is indicative of the ring opening of the glucosamine moiety. Taken together, these results support our view that the reductant $Na_2S_2O_4$ triggered the macroscopic gel-to-sol transition of the **GlcN-NPmoc** hydrogel through the reduction of the nitro group and the subsequent removal of the NPmoc group from **GlcN-NPmoc** via 1,6-elimination,[7g,15] which eventually induced the disassembly of the supramolecular architectures (gel degradation) due to the conversion of the supramolecular hydrogelator **GlcN-NPmoc** into

non-self-assembling molecules. All the components of this complex mixture are not fully assigned yet (**Figure 4D**).

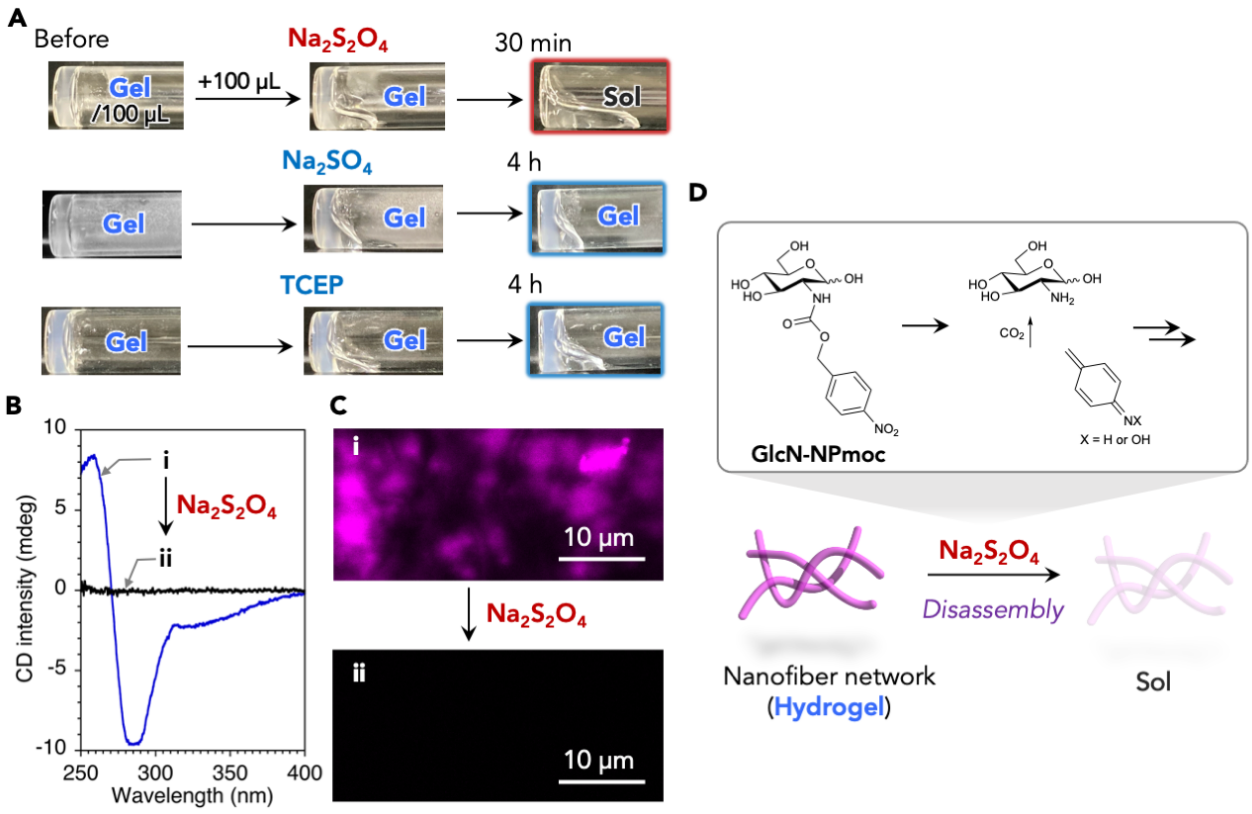

Figure 4. (**A**) Photographs of **GlcN-NPmoc** hydrogels [1.0 wt% (28 mM), 100 mM HEPES–NaOH (pH 7.4), 100 µL] before and after the addition of aqueous solutions (100 µL) containing $Na_2S_2O_4$ or Na_2SO_4 (20 eq.) or TCEP (1.0 eq.) as external stimuli at room temperature. (**B**) CD spectra and (**C**) CLSM images of the **GlcN-NPmoc** hydrogel [1.0 wt% (28 mM), 100 mM HEPES–NaOH (pH 7.4)] (**i**) before and (**ii**) after the addition of $Na_2S_2O_4$ (20 eq.) at room temperature. (**D**) Scheme showing the $Na_2S_2O_4$-responsive gel-to-sol transition of the **GlcN-NPmoc** hydrogel and the corresponding chemical transformation of the **GlcN-NPmoc** molecule.

CONCLUSION

In summary, we developed a glucosamine-based supramolecular hydrogelator capable of spontaneously forming supramolecular nanofibers via aqueous self-assembly, producing a reduction-responsive supramolecular hydrogel. This compact but modular molecularly designed hydrogelator, which can be synthesized in only one step using two commercially available compounds as the minimal starting materials, is one of the simplest low-molecular-weight supramolecular hydrogelators affording reduction-responsive supramolecular hydrogels.

The robustness of the present modular molecular design[20] and its synthetic simplicity could enable further development of various reduction-responsive aqueous nano- and soft-materials with improved properties and functions. For example, the properties and functions of supramolecular microspheres of galactosamine-based molecules should be further explored; however, this is beyond the scope of this paper focusing on supramolecular hydrogels. Furthermore, bioapplications of stimuli-responsive supramolecular hydrogels, such as in regenerative medicine and cosmetics, may become a target of research in the near future.

CONFLICTS OF INTEREST

The authors declare no conflicts of interest.

ACKNOWLEDGEMENTS

This work was supported in part by financial support from KOSÉ Cosmetology Research Foundation. S.L.H. thanks JSPS Research Fellowship for Young Scientists. The authors thank Mr. Koichiro M. Hirosawa and Prof. Kenichi G.N. Suzuki for their kind permission to use the CLSM facility and support. The authors acknowledge Life Science Research Center and Research Equipment Sharing Promotion Center, Gifu University for the maintenance of the instruments and their kind support. The authors would like to thank Enago (www.enago.jp) for the English language review.

REFERENCES

(1) (a) Estroff, L. A.; Hamilton, A. D. Water Gelation by Small Organic Molecules. *Chem. Rev.* **2004**, *104*, 1201–1218. (b) de Loos, M.; Feringa, B. L.; van Esch, J. H. Design and Application of Self-Assembled Low Molecular Weight Hydrogels. *Eur. J. Org. Chem.* **2005**, 3615–3631. (c) Du, X.; Zhou, J.; Shi, J.; Xu, B. Supramolecular Hydrogelators and Hydrogels: From Soft Matter to Molecular Biomaterials. *Chem. Rev.* **2015**, *115*, 13165–13307. (d) Draper, E. R.; Adams, D. J. Low-Molecular-Weight Gels: The State of the Art. *Chem* **2017**, *3*, 390–410. (e) Shigemitsu, H.; Hamachi, I. Design Strategies of Stimuli-Responsive Supramolecular Hydrogels Relying on Structural Analyses and Cell-Mimicking Approaches. *Acc. Chem. Res.* **2017**, *50*, 740–750. (f) Gelain, F.; Luo, Z.; Zhang, S. Self-Assembling Peptide EAK16 and RADA16 Nanofiber Scaffold Hydrogel. *Chem. Rev.* **2020**, *120*, 13434–13460.

(2) Li, Y.; Wang, F.; Cui, H. Peptide-based Supramolecular Hydrogels for Delivery of Biologics. *Bioengineering & Translational Medicine* **2016**, *1*, 306–322.

(3) Ikeda, M.; Ochi, R.; Hamachi, I. Supramolecular Hydrogel-Based Protein and Chemosensor Array. *Lab Chip* **2010**, *10*, 3325–3334.

(4) (a) Dou, X.-Q.; Feng, C.-L. Amino Acids and Peptide-Based Supramolecular Hydrogels for

Three-Dimensional Cell Culture. *Adv. Mater.* **2017**, *29*, 1604062. (b) He H.; Xu, B. Instructed-Assembly (iA): A Molecular Process for Controlling Cell Fate. *Bull. Chem. Soc. Jpn.* **2018**, *91*, 900–906. (c) Maruyama, T.; Restu, W. K. Intracellular Self-Assembly of Supramolecular Gelators to Selectively Kill Cells of Interest. *Polym. J.* **2020**, *52*, 883–889.

(5) Raeburn, J.; Cardoso, A. Z.; Adams, D. J. The Importance of The Self-Assembly Process to Control Mechanical Properties of Low Molecular Weight Hydrogels. *Chem. Soc. Rev.* **2013**, *42*, 5143–5156.

(6) (a) Matsumoto, S.; Yamaguchi, S.; Ueno, S.; Komatsu, H.; Ikeda, M.; Ishizuka, K.; Iko, Y.; Tabata, K.; Aoki, H.; Ito, S.; Noji, H.; Hamachi, I. Photo Gel-Sol/Sol-Gel Transition and Its Patterning of a Supramolecular Hydrogel as Stimuli-Responsive Biomaterials. *Chem. Eur. J.* **2008**, *14*, 3977–3986. (b) Larik, F. A.; Fillbrook, L. L.; Nurttila, S. S.; Martin, A. D; Kuchel, R. P.; Al Taief, K.; Bhadbhade, M.; Beves, J. E.; Thordarson, P. Ultra-Low Molecular Weight Photoswitchable Hydrogelators. *Angew. Chem. Int. Ed.* **2021**, DOI: 10.1002/anie.202015703.

(7) (a) Weiss, R. G.; Terech, P. Molecular Gels: Materials with Self-Assembled Fibrillar Networks Ch. 17, Ch. 18 (Springer: 2006). (b) Menger, F. M.; Caran, K. L. Anatomy of a Gel. Amino Acid Derivatives That Rigidify Water at Submillimolar Concentrations. *J. Am. Chem. Soc.* **2000**, *122*, 11679–11691. (c) Wojciechowski, J. P.; Martin, A. D.; Thordarson, P. Kinetically Controlled Lifetimes in Redox-Responsive Transient Supramolecular Hydrogels. *J. Am. Chem. Soc.* **2018**, *140*, 2869–2874. (d) Li, X.; Li, J.; Gao, Y.; Kuang, Y.; Shi, J.; Xu, B. Molecular Nanofibers of Olsalazine Form Supramolecular Hydrogels for Reductive Release of an Anti-inflammatory Agent. *J. Am. Chem. Soc.* **2010**, *132*, 17707–17709. (e) Sun, Z.; Li, Z.; He, Y.; Shen, R.; Deng, L.; Yang, M.; Liang, Y.; Zhang, Y. Ferrocenoyl Phenylalanine: A New Strategy Toward Supramolecular Hydrogels with Multistimuli Responsive Properties. *J. Am. Chem. Soc.* **2013**, *135*, 13379–13386. (f) Miao, X.; Cao, W.; Zheng, W.; Wang, J.; Zhang, X.; Gao, J.; Yang, C.; Kong, D.; Xu, H.; Wang, L.; Yang, Z. Switchable Catalytic Activity: Selenium-Containing Peptides with Redox-Controllable Self-Assembly Properties. *Angew. Chem. Int. Ed.* **2013**, *52*, 7781–7785. (g) Ikeda, M.; Tanida, T.; Yoshii, T.; Hamachi, I. Rational Molecular Design of Stimulus-Responsive Supramolecular Hydrogels Based on Dipeptides. *Adv. Mater.* **2011**, *23*, 2819–2822.

(8) Wilson, W.; Hay, M. Targeting Hypoxia in Cancer Therapy. *Nat. Rev. Cancer.* **2011**, *11*, 393–410.

(9) For recent reviews: (a) Gronwald, O.; Shinkai, S. Sugar-Integrated Gelators of Organic Solvents. *Chem. Eur. J.* **2001**, *7*, 4328–4334. (b) Datta, S.; Bhattacharya, S. Multifarious Facets of Sugar-Derived Molecular Gels: Molecular Features, Mechanisms of Self-Assembly and Emerging Applications. *Chem. Soc. Rev.* **2015**, *44*, 5596–5637. (c) Delbianco, M.; Bharate, P.; Varela-Aramburu, S.; Seeberger, P. H. Carbohydrates in Supramolecular Chemistry. *Chem. Rev.* **2016**, *116*, 1693−1752.

(10) (a) Fuhrhop, J. H.; Schnieder, P.; Rosenberg, J.; Boekema, E. The Chiral Bilayer Effect Stabilizes Micellar

Fibers. *J. Am. Chem. Soc.* **1987**, *109*, 3387–3390. (b) Jung, J. H.; Shinkai, S.; Shimizu, T. Spectral Characterization of Self-Assemblies of Aldopyranoside Amphiphilic Gelators: What is the Essential Structural Difference between Simple Amphiphiles and Bolaamphiphiles?. *Chem. Eur. J.* **2002**, *8*, 2684–2690. (c) Friggeri, A.; Gronwald, O.; van Bommel, K. J. C.; Shinkai, S.; Reinhoudt, D. N. Charge-Transfer Phenomena in Novel, Dual-Component, Sugar-Based Organogels. *J. Am. Chem. Soc.* **2002**, *124*, 10754–10758. (d) Kiyonaka, S.; Sugiyasu, K.; Shinkai, S.; Hamachi, I. First Thermally Responsive Supramolecular Polymer Based on Glycosylated Amino Acid. *J. Am. Chem. Soc.* **2002**, *124*, 10954–10955. (e) Roytman, R.; Adler-Abramovich, L.; Kumar, K. S. A.; Kuan, T.-C.; Lin, C.-C.; Gazit, E.; Brik, A. Exploring the Self-Assembly of Glycopeptides Using a Diphenylalanine Scaffold. *Org. Biomol. Chem.* **2011**, *9*, 5755–5761. (f) Clemente, M. J.; Fitremann, J.; Mauzac, M.; Serrano, J. L.; Oriol, L. Synthesis and Characterization of Maltose-Based Amphiphiles as Supramolecular Hydrogelators. *Langmuir* **2011**, *27*, 15236–15247. (g) Ikeda, M.; Ochi, R.; Kurita, Y.-s.; Pochan, D. J.; Hamachi, I. Heat-Induced Morphological Transformation of Supramolecular Nanostructures by Retro-Diels‑Alder Reaction. *Chem. Eur. J.* **2012**, *18*, 13091–13096. (h) Ochi, R.; Kurotani, K.; Ikeda, M.; Kiyonaka, S.; Hamachi, I. Supramolecular Hydrogels Based On Bola-Amphiphilic Glycolipids Showing Color Change in Response to Glycosidases. *Chem. Commun.* **2013**, *49*, 2115–2117. (i) Latxague, L.; Ramin, M.A.; Appavoo, A.; Berto, P.; Maisani, M.; Ehret, C.; Chassande, O.; Barthélémy, P. Control of Stem-Cell Behavior by Fine Tuning the Supramolecular Assemblies of Low-Molecular-Weight Gelators. *Angew. Chem. Int. Ed.* **2015**, *54*, 4517–4521. (j) Liu, J.; Sun, Z.; Yuan, Y.; Tian, X.; Liu, X.; Duan, G.; Yang, Y.; Yuan, L.; Lin, H.-C.; Li, X. Peptide Glycosylation Generates Supramolecular Assemblies from Glycopeptides as Biomimetic Scaffolds for Cell Adhesion and Proliferation. *ACS Appl. Mater. Interfaces* **2016**, *8*, 6917–6924. (k) Tsuzuki, T.; Kabumoto, M.; Arakawa, H.; Ikeda, M. The Effect of Carbohydrate Structures on The Hydrogelation Ability and Morphology of Self-Assembled Structures of Peptide–Carbohydrate Conjugates in Water. *Org. Biomol. Chem.* **2017**, *15*, 4595–4600. (l) Akama, S.; Maki, T.; Yamanaka, M. Enzymatic Hydrolysis-Induced Degradation of a Lactose-Coupled Supramolecular Hydrogel. *Chem. Commun.* **2018**, *54*, 8814–8817. (m) Restuccia, A.; Seroski, D. T.; Kelley, K. L.; O'Bryan, C. S.; Kurian, J. J.; Knox, K. R.; Farhadi, S. A.; Angelini, T. E.; Hudalla, G. A. Hierarchical Self-Assembly and Emergent Function of Densely Glycosylated Peptide Nanofibers. *Commun. Chem.* **2019**, *2*, 53. (n) Biswakarma, D.; Deya, N.; Bhattacharya, S. A Thermo-Responsive Supramolecular Hydrogel That Senses Cholera Toxin via Color-Changing Response. *Chem. Commun.* **2020**, *56*, 7789–7792. (o) He, C.; Wu, S.; Liu, D.; Chi, C.; Zhang, W.; Ma, M.; Lai, L.; Dong, S. Glycopeptide Self-Assembly Modulated by Glycan Stereochemistry through Glycan–Aromatic Interactions. *J. Am. Chem. Soc.* **2020**, *142*, 17015–17023.

(11) Gama, C. I.; Hsieh-Wilson, L. C. Chemical Approaches to Deciphering the Glycosaminoglycan Code. *Curr.*

Opin. Chem. Biol. **2005**, *9*, 609–619.

(12) (a) Yang, Z.; Liang, G.; Ma, M.; Abbah, A. S.; Lu, W. W.; Xu, B. D-Glucosamine-based Supramolecular Hydrogels to Improve Wound Healing. *Chem. Commun.* **2007**, 843–845. (b) Wang, G.; Cheuk, S.; Yang, H.; Goyal, N.; Narasimha Reddy, P. V.; Hopkinsonm, B. Synthesis and Characterization of Monosaccharide-Derived Carbamates as Low-Molecular-Weight Gelators. *Langmuir* **2009**, *25*, 8696–8705.

(13) (a) Birchall, L. S.; Roy, S.; Jayawarna, V.; Hughes, M.; Irvine, E.; Okorogheye, G. T.; Saudi, N.; De Santis, E.; Tuttle, T.; Edwards, A. A.; Ulijn, R. V. Exploiting CH-π Interactions in Supramolecular Hydrogels of Aromatic Carbohydrate Amphiphiles. *Chem. Sci.* **2011**, *2*, 1349–1355. (b) Pires, R. A.; Abul-Haija, Y. M.; Costa, D. S.; Novoa-Carballal, R.; Reis, R. L.; Ulijn, R. V.; Pashkuleva, I. Controlling Cancer Cell Fate Using Localized Biocatalytic Self- Assembly of an Aromatic Carbohydrate Amphiphile. *J. Am. Chem. Soc.* **2015**, *137*, 576–579.

(14) Very recently, Singh *et al*.[14a] reported that the addition of aqueous $Na_2S_2O_4$ to a hydrogel constructed from a monosaccharide-based supramolecular hydrogelator bearing an aldehyde group (M_w = 310.30 g/mol)[14b] induced macroscopic gel-to-sol transition.[14a] It was therein demonstrated that the aldehyde is converted into a hydrophilic α-hydroxy sulfonate through reversible nucleophilic addition of a bisulfite anion (HSO_3^-), which is spontaneously generated by fragmentations of $S_2O_4^{2-}$ in an aqueous solution, to the aldehyde.[14a,c,d] In fact, there is a discrepancy between ref 14a (α-hydroxy sulfonate produced by reaction between aldehyde and HSO_3^-) and ref 14d (α-hydroxy sulfinate produced by the reaction between aldehyde and HSO_2^-) for the intermediate of the complete reduction of aldehyde to alcohol by $Na_2S_2O_4$. Nevertheless, to the best of our knowledge, this may be the lowest molecular weight hydrogelator[14a,b] exhibiting reductant responsiveness among the previously reported examples (**Figure S1**). (a) Singh, N.; Lainer, B.; Formon, G. J. M.; De Piccoli, S.; Hermans, T. M. Re-programming Hydrogel Properties Using a Fuel-Driven Reaction Cycle. *J. Am. Chem. Soc.* **2020**, *142*, 4083–4087. (b) Chen, Q.; Lv, Y.; Zhang, D.; Zhang, G.; Liu, C.; Zhu, D. Cysteine and pH-Responsive Hydrogel Based on a Saccharide Derivative with an Aldehyde Group. *Langmuir* **2010**, *26*, 3165–3168. (c) Kjell, D. P.; Slattery, B. J.; Semo, M. J. A Novel, Nonaqueous Method for Regeneration of Aldehydes from Bisulfite Adducts. *J. Org. Chem.* **1999**, *64*, 5722−5724. (d) de Vries, J. G.; Kellogg, R. M. Reduction of Aldehydes and Ketones by Sodium Dithionite. *J. Org. Chem.* **1980**, *45*, 4126−4129.

(15) Qian, X.; Hindsgaul, O. Use of the *p*-Nitrobenzyloxycarbonyl Group as an Orthogonal Amine Protecting Group in the Synthesis of β-GlcNAc Terminating Glycosides. *Chem. Commun.* **1997**, 1059–1060.

(16) Yan, C.; Pochan, D. J. Rheological Properties of Peptide-Based Hydrogels for Biomedical and Other Applications. *Chem. Soc. Rev.* **2010**, *39*, 3528–3540.

(17) Tao, K.; Levin, A.; Adler-Abramovich, L.; Gazit, E. Fmoc-modified Amino Acids and Short Peptides: Simple Bio-Inspired Building Blocks for the Fabrication of Functional Materials. *Chem. Soc. Rev.* **2016**, *45*,

3935–3953.

(18) Uzu, S.; Kanda, S.; Imai, K.; Nakashima, K.; Akiyama, S. Fluorogenic Reagents: 4-Aminosulphonyl-7-hydrazino-2,1,3-benzoxadiazole, 4-(*N*,*N*-DimethylaminosuIphonyl)-7-hydrazino-2,1,3-benzoxadiazole and 4-Hydrazino-7-nitro-2,1,3-benzoxadiazole Hydrazine for Aldehydes and Ketones, *Analyst* **1990**, *115*, 1477–1482.

(19) (a) Sreenivasachary, N.; Lehn, J.-M. Gelation-driven Component Selection in the Generation of Constitutional Dynamic Hydrogels Based on Guanine-Quartet Formation. *Proc. Natl. Acad. Sci. USA* **2005**, *102*, 5938–5943. (b) Corbett, P. T.; Leclaire, J.; Vial, L.; R. West, K.; Wietor, J.-L.; Sanders, J. K. M.; Otto, S. Dynamic Combinatorial Chemistry. *Chem. Rev*. **2006**, *106*, 3652–3711. (c) Reuther, J. F.; Dahlhauser, S. D.; Anslyn, E. V. Tunable Orthogonal Reversible Covalent (TORC) Bonds: Dynamic Chemical Control over Molecular Assembly. *Angew. Chem. Int. Ed.* **2019**, *58*, 74–85. (d) Kubota, R.; Nagao, K.; Tanaka, W.; Matsumura, R.; Aoyama, T.; Urayama, K.; Hamachi, I. Control of Seed Formation Allows Two Distinct Self-Sorting Patterns of Supramolecular Nanofibers. *Nat. Commun*. **2020**, *11*, 4100.

(20) Ikeda, M. Stimuli-responsive Supramolecular Systems Guided by Chemical Reactions. *Polym. J*. **2019**, *51*, 371–380.

Supporting Information

Development of an amino sugar-based supramolecular hydrogelator with reduction responsiveness

Sayuri L. Higashi[1] and Masato Ikeda[1,2,3,4,5]*

[1] *United Graduate School of Drug Discovery and Medical Information Sciences, Gifu University, 1-1 Yanagido, Gifu 501-1193, Japan*
[2] *Department of Chemistry and Biomolecular Science, Faculty of Engineering, Gifu University, 1-1 Yanagido, Gifu 501-1193, Japan*
[3] *Center for Highly Advanced Integration of Nano and Life Sciences, Gifu University (G-CHAIN), 1-1 Yanagido, Gifu 501-1193, Japan*
[4] *Institute of Nano-Life-Systems, Institutes of Innovation for Future Society, Nagoya University, Furo-cho, Chikusa-ku, Nagoya, 464-8603, Japan*
[5] *Institute for Glyco-core Research (iGCORE), Gifu University, Furo-cho, Chikusa-ku, Nagoya, 464-8603, Japan*

* *Correspondence: m_ikeda@gifu-u.ac.jp, orcid.org/0000-0003-4097-829*

Contents:

Experimental

Generals Unless stated otherwise, all commercial reagents were used as received. Water used in the experiments refers to ultra-pure water obtained from a Millipore system having a specific resistance of 18 MΩ•cm. Thin layer chromatography (TLC) was performed on silica gel $60F_{254}$ (Merck). Column chromatography was performed on silica gel PSQ-100B (Fuji Silysia Chemical, 100 μm). ^{1}H and ^{13}C NMR spectra were obtained on a JEOL JNM ECS-400 spectrometer (400 MHz for ^{1}H, 100 MHz for ^{13}C) with tetramethylsilane (TMS) or residual non-deuterated solvents (internal 1,4-dioxane or DMSO for D_2O) as the internal references. Multiplicities are abbreviated as follows: s = singlet, d = doublet, t = triplet, q = quartet, m = multiplet, dd = double doublet, br = broad. ESI mass spectrometry was performed on a JEOL JMS-T100LP AccuTOF LC-plus mass spectrometer.

Conventional hydrogelation ability test: Gelation ability was evaluated by an inverted tube test. Typically, a DMSO stock solution of **GlcN-NPmoc** (200 mg/mL, 10 μL) was mixed with 100 mM HEPES-NaOH buffer (pH 7.4, 190 μL) to obtain an aqueous dispersion (1.0 wt%, 28 mM) in a glass vial. The resultant solution was applied with sonication and heated by a heat gun. When a transparent aqueous solution was obtained, the solution was cooled down at room temperature for designated time and the hydrogel formation was evaluated by inverting the glass vial.

Rheological measurement: Dynamic frequency and strain sweep experiments were carried out on a TA instruments AR-G2 rheometer using a 20-mm stainless steel parallel plate (The temperature of the plate was controlled at 25 °C by Peltier system) at the gap of 1.5 mm. Hydrogel samples were placed on the plate. All the gels showed almost linear viscoelastic regime up to 1.0% strain (frequency: 1.0 rad/s). Therefore, frequency sweep (0.1–100 rad/s) was performed under 0.20 % strain.

TEM observation: Sample (ca. 10 μL) was dropped on a copper TEM grid covered by an elastic carbon-support film (20–25 nm) with a filter paper underneath and the excess solution was blotted with the filter paper immediately. The TEM grid was dried under a reduced pressure for at least 6 h prior to TEM observation. TEM images were acquired using a Hitachi H-7000 (accelerating voltage: 100 kV) equipped with a CCD camera and analyzed with Fiji (freely available at https://fiji.sc./)[S1,S2] on a Macintosh PC.

Circular dichroism (CD) spectroscopy: CD spectra were recorded in a 0.1-mm quartz cell unless otherwise noted on a Jasco J-820 spectropolarimeter equipped with a programmable temperature-control unit (Julabo HP-4). The spectra were obtained by using a 2-nm slit width and a scanning step of 0.1 nm from 400 to 250 nm. Each spectrum was an average of 4 scans with the solvent background subtracted.

Infrared (IR) spectroscopy: Fourier transform (FT) IR spectra were acquired using a Shimadzu IRAffinity-1 spectrometer with a spectral resolution of 4 cm^{-1}. The spectra were obtained by averaging 128 scans for each sample with the solvent background subtracted. Hydrogels prepared with D_2O were sandwiched directly between CaF_2 windows (32 × 3 mm) separated by a 100 μm PTFE spacer.

CLSM observation: A **GlcN-NPmoc** hydrogel or a **GalN-NPmoc** dispersion [1.0 wt%, 100 mM HEPES-NaOH (pH 7.4, 10 μL) or 50 mM MES-NaOH (pH 5.5, 10 μL) containing DMSO (5.0 vol%)] obtained according to the procedure described above was mixed with an aqueous DMSO (2.0 vol%) solution of Nile Red (600 μM, 1.0 μL) or a DMSO solution of NBD-H (50 mM, 1.0 μL) and spotted on a glass coverslip (diameter: 25 mm, thickness: 0.13–0.17 mm, Fisher Scientific) placed in Attofluor cell chamber (Thermo Fisher Scientific) with water drops (ca. 50 μL) around the sample drop to avoid dryness. Confocal laser scanning fluorescence microscopy (CLSM) observations were performed with an FV1000-D microscope (IX81, Olympus) equipped with a LED laser (559 nm) for Nile Red, an Ar laser (488 nm) for NBD, and a Gallium Arsenide Phosphide (GaAsP) detector. A 60× (numerical aperture (NA) = 1.49) oil objective was employed to obtain images (typically, 1024 × 1024 pixel). The images were obtained and analyzed by the acquisition software FV10-ASW4.2 equipped with the microscope.

Reduction-responsive gel-to-sol transition of GlcN-NPmoc hydrogel: Typically, to a **GlcN-NPmoc** hydrogel [1.0 wt%, 100 mM HEPES-NaOH (pH 7.4, 200 μL) containing DMSO (5.0 vol%)] was added an aqueous solution of $Na_2S_2O_4$ (1.1 M, 100 μL, 20 eq.) and the resultant sample was incubated at room temperature for designated time. Stimuli-responsive gel-to-sol transition was carefully evaluated by an inverted tube test. As negative control experiments, an aqueous solution of Na_2SO_4 (1.1 M, 100 μL, 20 eq.) or TCEP (56 mM, 100 μL, 1 eq.) was added instead of the aqueous solution of $Na_2S_2O_4$.

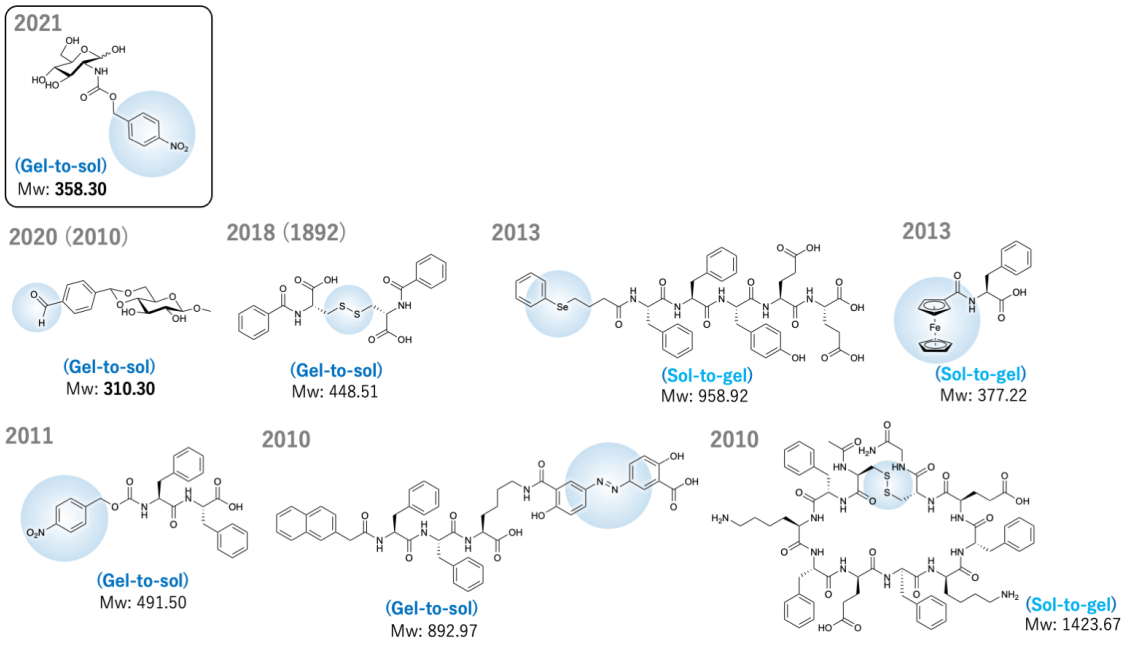

Figure S1 Chemical structures of representative supramolecular hydrogelators capable of producing reduction-responsive or reductant-responsive supramolecular hydrogels (references 7 and 14a,b in main text).

Synthesis

Synthesis of NPmoc-carbohydrates (GlcN- and GalN-NPmoc)

Synthetic scheme (**Scheme S1**) for NPmoc-carbohydrates (**GlcN-** and **GalN-NPmoc**) from amino sugars was shown below.[S3]

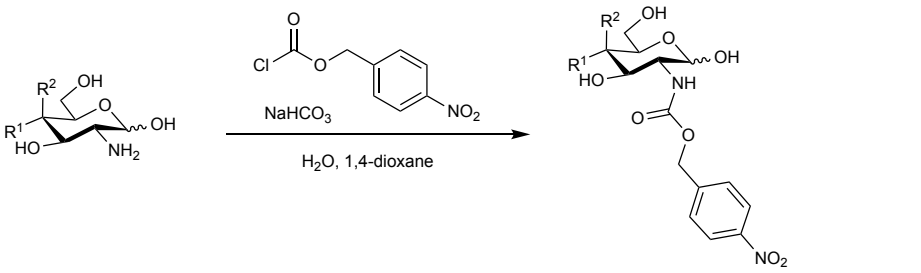

Scheme S1. Synthesis of NPmoc-carbohydrates (**GlcN-** and **GalN-NPmoc**).

Synthesis of GlcN-NPmoc: To a solution of **GlcNH$_2$ • HCl** (50 mg, 0.23 mmol) in H_2O (1.0 mL) was added $NaHCO_3$ (39 mg, 0.46 mol). The mixture was cooled on ice bath and a freshly prepared solution of NPmoc-Cl (**Scheme S1**, 60 mg, 0.28 mmol) in 1,4-dioxane (0.50 mL) was added dropwise. Further 1,4-dioxane (0.83 mL) and H_2O (0.50 mL) were added to the mixture and the resultant mixture was stirred for 1.5 h at room temperature. Then, the solvents were removed by evaporation and to the resulting residue was added CH_2Cl_2 (5 mL). A precipitate formed was collected by filtration, washed with CH_2Cl_2 (15 mL) and H_2O (5 mL), and dried *in vacuo* to give **GlcN-NPmoc** (61 mg, 74%) as a white solid. TLC: R_f = 0.32 [ethyl acetate:methanol:water = 28:2:1 (*v/v/v*)]; ^{1}H NMR (DMSO-d_6 + D_2O, 400 MHz, rt): δ (ppm) = 8.24 (d, J_H = 8.0 Hz, Ar*H*, 2H), 7.63 (d, J_H = 8.8 Hz, Ar*H* , 2H), 7.14 (d, J_H = 8.0 Hz, slightly remained even after the addition of D_2O, N*H*, β-anomer), 6.50 (d, J_H = 4.8 Hz, slightly remained even after the addition of D_2O, N*H*, α-anomer), 5.15 (s, 2H), 4.96 (d, J_H = 3.2 Hz, 0.67H, ^{1}C*H*, α-anomer), 4.42 (d, J_H = 8.0 Hz, 0.32H, ^{1}C*H*, β-anomer), 3.67–3.03 (m, 6H, ^{2,3,4,5,6}C*H*), Duplicated signals distinguishable was assigned to the two anomeric forms.; ^{13}C NMR (DMSO-d_6, 100 MHz, rt): δ (ppm) = 56.67, 59.06, 61.28, 61.34, 64.22, 70.51, 71.07, 71.23, 72.27, 74.39, 77.03, 90.87, 95.56, 123.74, 128.34, 145.51, 147.10, 156.04; HRMS (ESI, positive): Calcd. for [M($C_{14}H_{18}N_2O_9$) + Na]$^+$: *m/z* = 381.0910; Found: 381.0894.

Synthesis of GalN-NPmoc: The titled compound was prepared from **GalNH$_2$ • HCl** (50 mg, 0.23 mmol) and NPmoc-Cl in the similar way for **GlcN-NPmoc** and was obtained in 57% yield (47 mg) as an off-white solid. TLC: R_f = 0.30 [ethyl acetate:methanol:water = 28:2:1 (*v/v/v*)]; ^{1}H NMR (DMSO-d_6 + D_2O, 400 MHz, rt): δ (ppm) = 8.22 (d, J_H = 8.0 Hz, Ar*H*, 2H), 7.61 (d, J_H = 8.0 Hz, Ar*H*, 2H), 6.98 (d, J_H = 8.8 Hz, remained even after the addition of D_2O, N*H*, β-anomer), 6.43 (d, J_H = 8.4 Hz, remained even after the addition of D_2O, N*H*, α-anomer), 5.14 (d, J_H = 2.4 Hz, 2H), 4.94 (d, J_H = 3.2 Hz, 0.47H, ^{1}C*H*, α-anomer), 4.36 (d, J_H = 7.6 Hz, 0.17H, ^{1}C*H*, β-anomer), 3.81–3.43 (m, 6H, ^{2,3,4,5,6}C*H*), Duplicated signals distinguishable was assigned to the two anomeric forms.; ^{13}C NMR (DMSO-d_6, 100 MHz, rt): δ (ppm) = 52.37, 60.57, 60.64, 63.81, 63.96, 64.21, 67.10, 67.67, 68.29, 70.47, 71.27, 75.08, 91.09, 123.52, 128.07, 145.37, 146.88, 155.97; HRMS (ESI, positive): Calcd. for [M($C_{14}H_{18}N_2O_9$) + Na]$^+$: *m/z* = 381.0910; Found: 381.0900.

Characterization of compounds

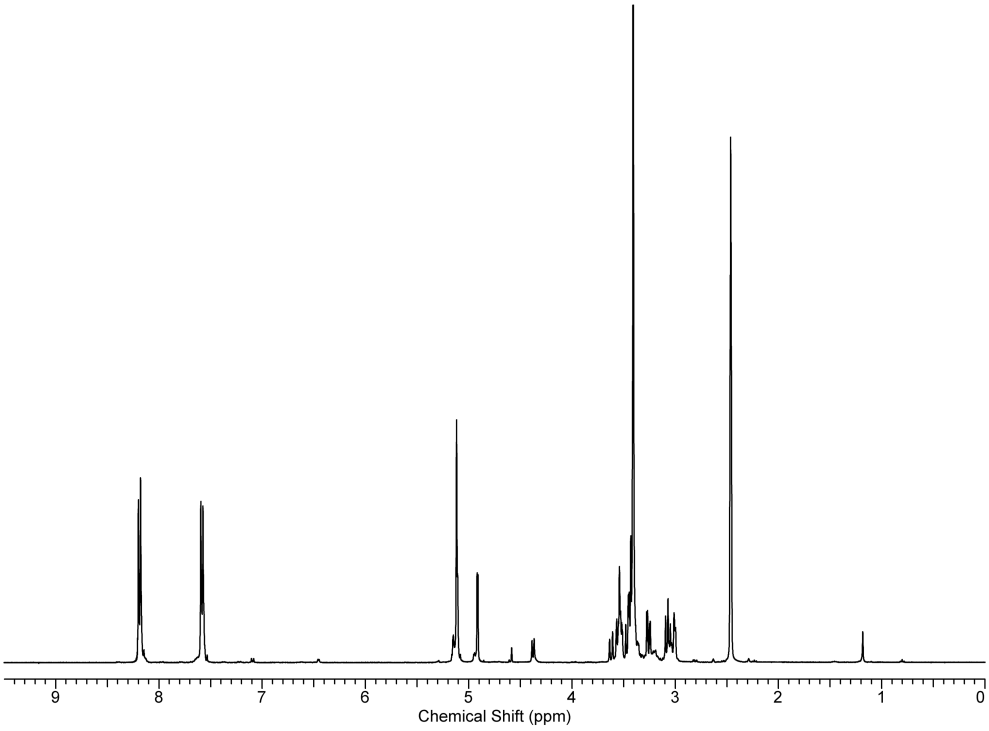

Figure S2. ^{1}H NMR spectrum (400 MHz, DMSO-d_6 + D_2O, rt) of **GlcN-NPmoc**.

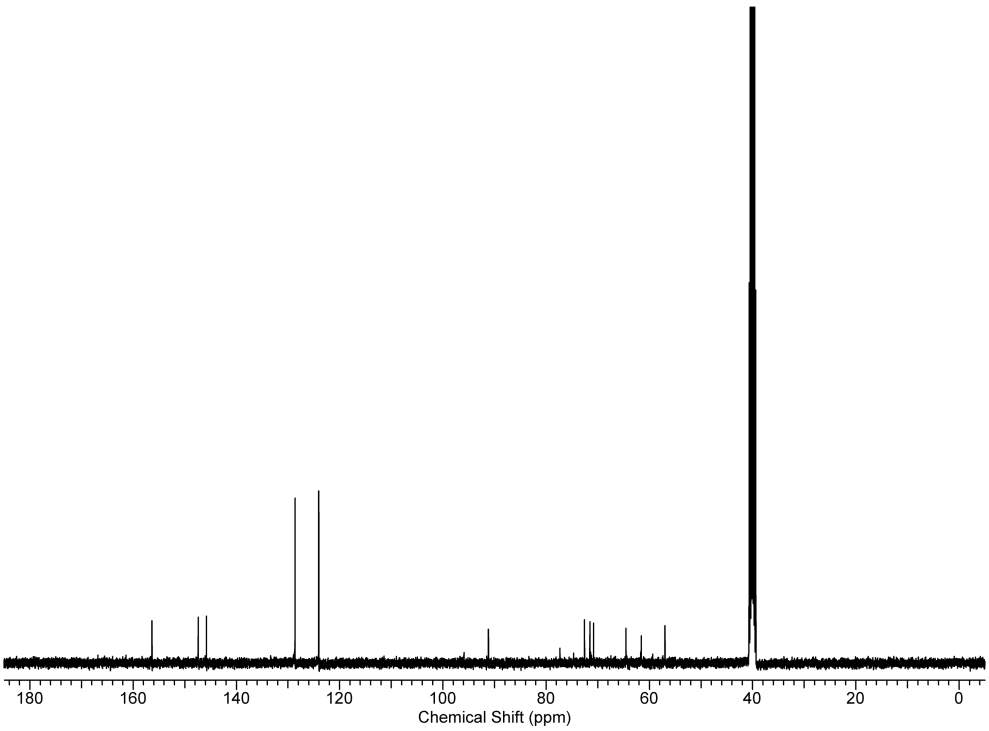

Figure S3. ^{13}C NMR spectrum (100 MHz, DMSO-d_6, rt) of **GlcN-NPmoc**.

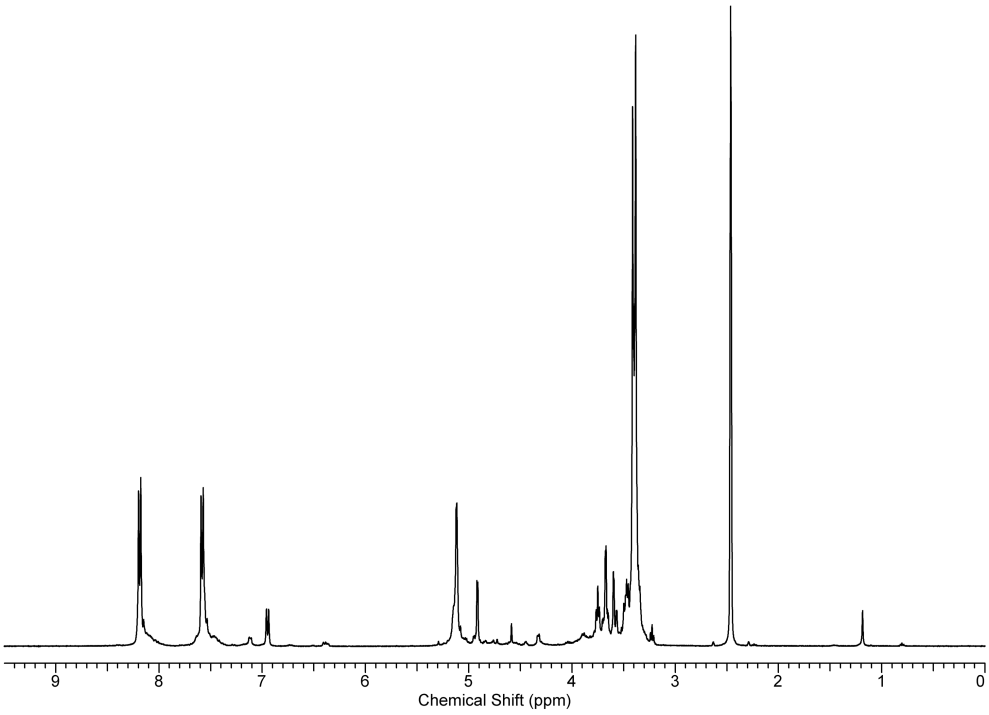

Figure S4. ^{1}H NMR spectrum (400 MHz, DMSO-d_6 + D_2O, rt) of **GalN-NPmoc**.

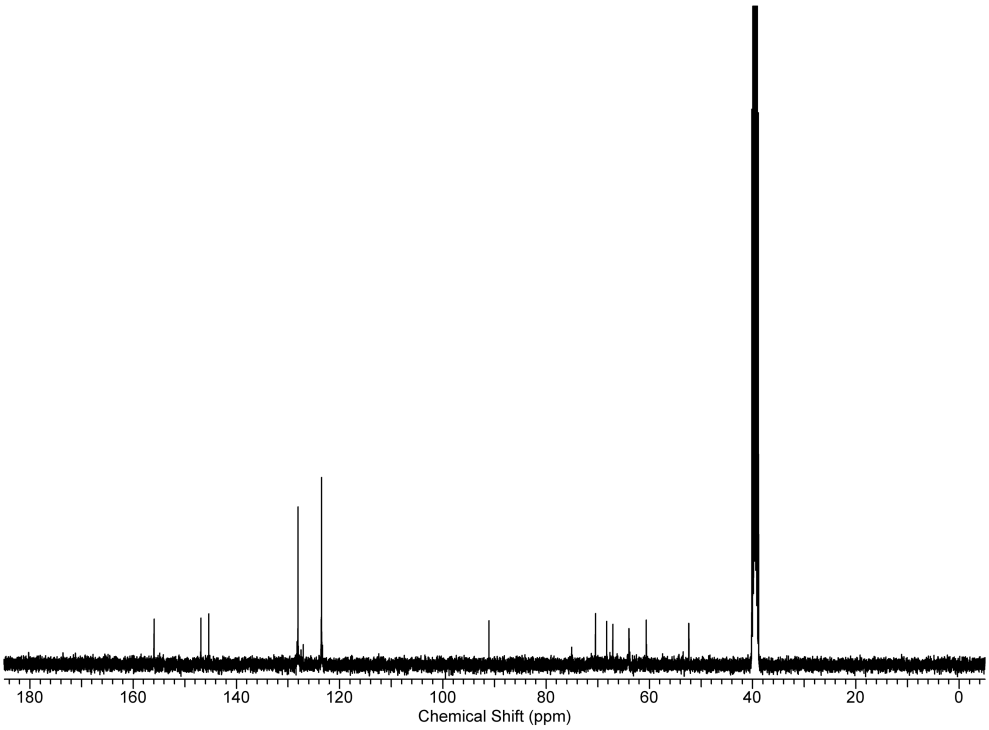

Figure S5. ^{13}C NMR spectrum (100 MHz, DMSO-d_6, rt) of **GalN-NPmoc**.

Characterization of supramolecular hydrogels

■Gelation ability of NPmoc-carbohydrates (GlcN- and GalN-NPmoc)

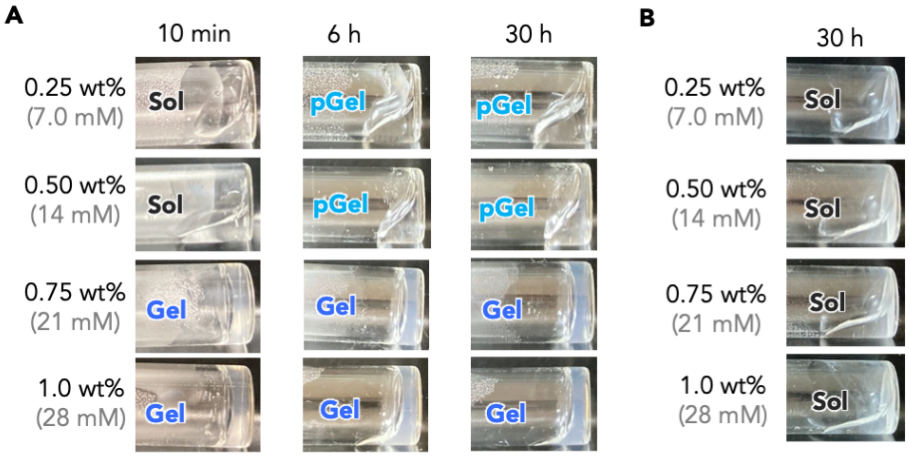

Figure S6. Photographs showing gelation ability of NPmoc-carbohydrates (**A**: **GlcN-** and **B**: **GalN-NPmoc**) [*Sol*: solution or dispersion (not gel), *pGel*: partial gel (solution flow was observed while a part of the solution was gelled), *Gel*: hydrogel (no solution flow)] at various concentrations. *Conditions*: [**GlcN-** or **GalN-NPmoc**] = 0.25, 0.50, 0.75, 1.0 wt%, 100 mM HEPES-NaOH (pH 7.4) containing DMSO (5.0 vol%), rt.

■Post-self-assembly functionalization of supramolecular architectures of NPmoc-carbohydrates

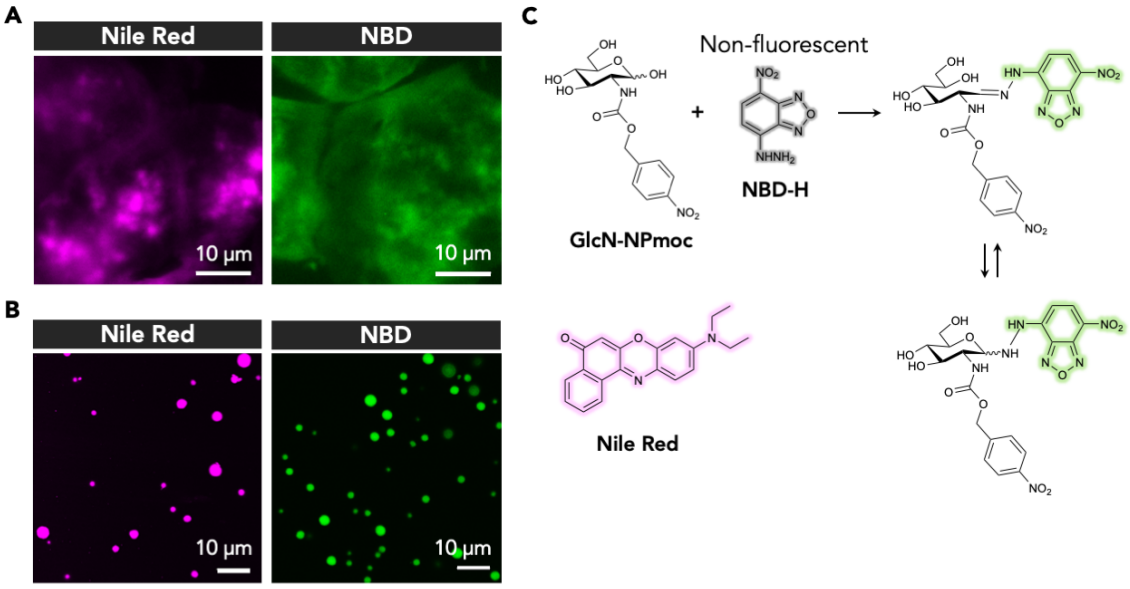

Figure S7. Representative CLSM images of (**A**) **GlcN-NPmoc** hydrogel and (**B**) **GalN-NPmoc** dispersion (sol) stained with Nile Red (left, magenta) or NBD-H (right, green). (**C**) Chemical structures of Nile Red and NBD-H and reaction scheme between **GlcN-NPmoc** (self-assembled or not) and NBD-H, which should give rise to fluorescent molecules through hydrazone bond formation. *Conditions:* [**GlcN-NPmoc** or **GalN-NPmoc**] = 0.91 wt% (26 mM), for Nile Red staining: [Nile Red] = 55 μM in an aqueous mixture (a:b = 10:1 (*v*/*v*)) of (a) 50 mM MES-NaOH (pH 5.5) containing DMSO (5.0 vol%) and (b) 50 mM MES-NaOH (pH 5.5) containing DMSO (2.0 vol%), or NBD staining: [NBD] = 4.5 mM in an aqueous mixture (a:b = 10:1 (*v*/*v*)) of (a) 50 mM MES-NaOH (pH 5.5) containing DMSO (5.0 vol%) and (b) DMSO, rt.

■CD spectral study of GlcN-NPmoc hydrogel

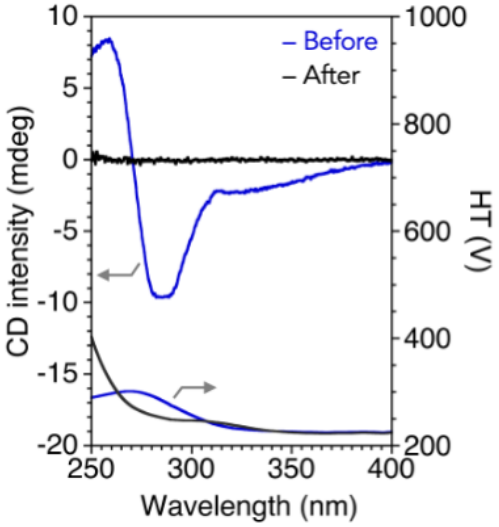

Figure S8. Circular dichroism (CD) spectra (*l* = 0.1 mm) of **GlcN-NPmoc** hydrogel and the corresponding HT voltage spectra before and 30 min after the addition of $Na_2S_2O_4$ (20 eq.). *Conditions*: [**GlcN-NPmoc**] = 1.0 wt% in MilliQ water (to avoid the influence of DMSO and HEPES on the spectra), rt.

■FTIR spectral study of GlcN-NPmoc hydrogel and NPmoc-containing water-soluble OEG-NPmoc

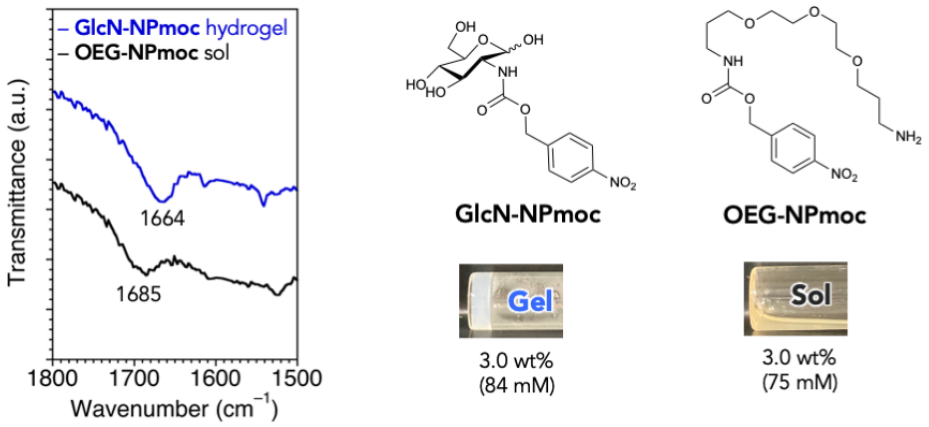

Figure S9. FTIR spectra of **GlcN-NPmoc** hydrogel and NPmoc-containing water-soluble **OEG-NPmoc** sol. (right) Chemical structures and photos of samples are shown. *Conditions*: [**GlcN-NPmoc**] = 3.0 wt% (84 mM), [**OEG-NPmoc**] = 3.0 wt% (75 mM), D_2O, rt.

■^{1}H NMR study of reduction-responsiveness of GlcN-NPmoc hydrogel

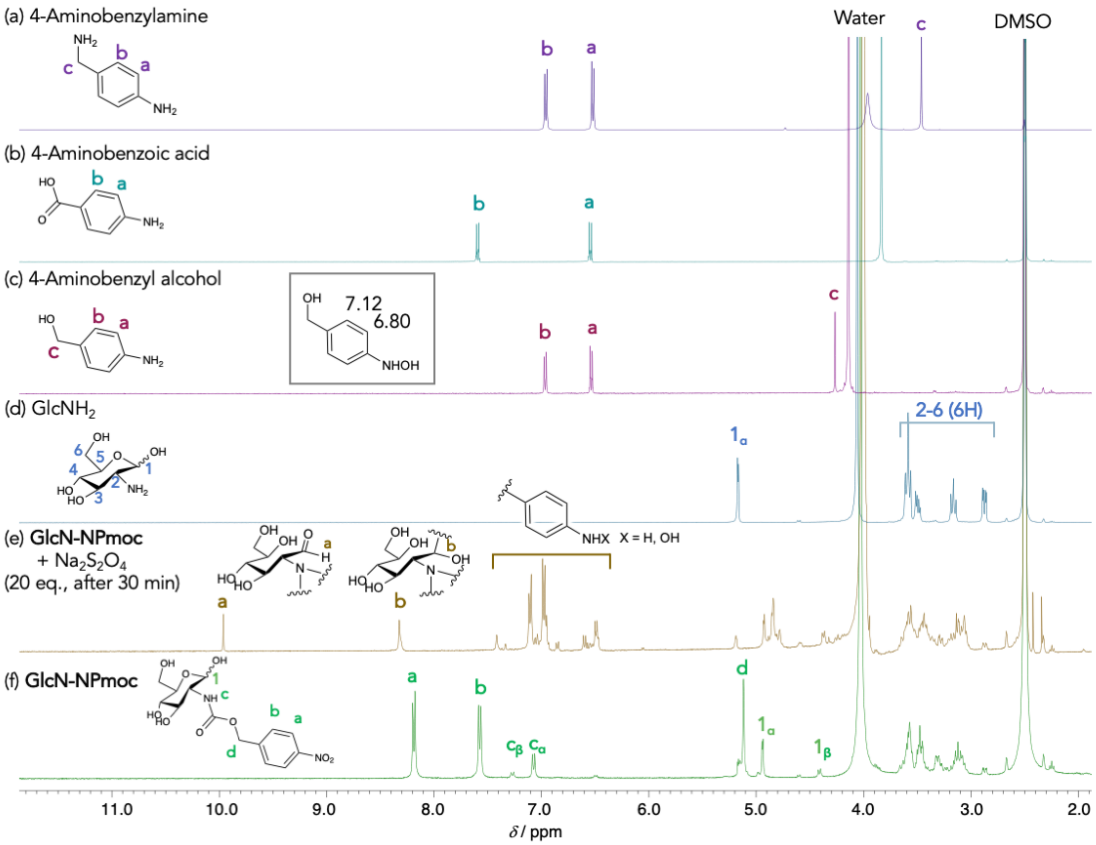

Figure S10. ^{1}H NMR spectra (400 MHz, rt) of (a) 4-aminobenzylamine, (b) 4-aminozenboic acid, (c) 4-aminobenzyl alcohol, (d) $GlcNH_2$ (D-glucosamine), and **GlcN-NPmoc** hydrogel (e) before and 30 min after the addition of $Na_2S_2O_4$ (20 eq.) For (e); To a **GlcN-NPmoc** hydrogel (1.0 wt%, 200 μL) prepared with D_2O was added a solution of $Na_2S_2O_4$ in D_2O (2.2 M, 50 μL) and the portion (100 μL) of resultant solution (after 30 min when gel-to-sol transition was verified) was diluted with DMSO-d_6 (600 μL). For (f); **GlcN-NPmoc** hydrogel (1.0 wt%, 100 μL) was dissolved by the addition of DMSO-d_6 (600 μL). Previously reported chemical shifts of 4-hydroxyaminobenzyl alcohol[S4] was shown in (c). *Conditions*: DMSO-d_6:D_2O = 1:6 (*v*/*v*), rt.

References

[S1] J. Schindelin, I. Arganda-Carreras, E. Frise, V. Kaynig, M. Longair, T. Pietzsch, S. Preibisch, C. Rueden, S. Saalfeld, B. Schmid, J.-Y. Tinevez, D. J. White, V. Hartenstein, K. Eliceiri, P. Tomancak and A. Cardona, Fiji: an open-source platform for biological-image analysis, *Nat. Methods*, 2012, **9**, 676–682.

[S2] C. T. Rueden, J. Schindelin, M. C. Hiner, B. E. DeZonia, A. E. Walter, E. T. Arena and K. W. Eliceiri, ImageJ2: ImageJ for the next generation of scientific image data, *BMC Bioinformatics*, 2017, **18**, 529.

[S3] L. S. Birchall, S. Roy, V. Jayawarna, M. Hughes, E. Irvine, G. T. Okorogheye, N. Saudi, E. De Santis, T. Tuttle, A. A. Edwards, R. V. Ulijn, Exploiting CH-π Interactions in supramolecular hydrogels of aromatic carbohydrate amphiphiles. *Chem. Sci.*, 2011, **2**, 1349–1355.

[S4] K. Tanaka, Y. Yamamoto, A. Kuzuya, M. Komiyama, Synthesis of photo-responsive acridine-modified DNA and its application to site-selective RNA scission. *Nucleosides Nucleotides Nucleic Acids*, 2008, **27**, 1175–1185.